

Generating Black-Box Adversarial Examples in Sparse Domain

Hadi Zanddizari

Department of Electrical Engineering
University of South Florida
Tampa, Florida, U.S.A
Email: hadiz@mail.usf.edu

J. Morris Chang

Department of Electrical Engineering
University of South Florida
Tampa, Florida, U.S.A
Email: chang5@usf.edu

Abstract—Applications of machine learning (ML) models and convolutional neural networks (CNNs) have been rapidly increased. Although state-of-the-art CNNs provide high accuracy in many applications, recent investigations show that such networks are highly vulnerable to adversarial attacks. The black-box adversarial attack is one type of attack that the attacker does not have any knowledge about the model or the training dataset, but it has some input data set and their labels.

In this paper, we propose a novel approach to generate a black-box attack in sparse domain whereas the most important information of an image can be observed. Our investigation shows that large sparse components play a critical role in the performance of the image classifiers. Under this presumption, to generate adversarial example, we transfer an image into a sparse domain and put a threshold to choose only k largest components. In contrast to the very recent works that randomly perturb k low frequency (LoF) components, we perturb k largest sparse (LaS) components either randomly (query-based) or in the direction of the most correlated sparse signal from a different class. We show that LaS components contain some middle or higher frequency components information which can help us fool the classifiers with a fewer number of queries. We also demonstrate the effectiveness of this approach by fooling the TensorFlow Lite (TFLite) model of Google Cloud Vision platform. Mean squared error (MSE) and peak signal to noise ratio (PSNR) are used as quality metrics. We present a theoretical proof to connect these metrics to the level of perturbation in the sparse domain. We tested our adversarial examples to the state-of-the-art CNNs and support vector machine (SVM) classifiers on color and grayscale image datasets. The results show the proposed method can highly increase the misclassification rate of the classifiers.

I. INTRODUCTION

By the ever-increasing demands for analyzing and processing large datasets, ML algorithms and particularly deep learning techniques have become the center of attention of many companies and service providers. The remarkable performance of CNNs for image segmentation, classification, and object tracking could provide acceptable solutions for many problems encountered in computer vision and biomedical engineering. [1], [2]. While almost CNNs perform well and provide high accuracy, but their robustness toward some malicious attacks still are not acceptable [3]–[5]. Applying some perturbation on the input data may totally undermine the high accuracy of a classifier. Because ML models are usually trained and deployed in benign settings. In other words, they do not

consider certain scenarios where an attacker can compromise the performance of the system.

Recently, many works have been proposed to point out the vulnerability of CNNs against adversarial scenarios [6]–[10]. By slightly perturbing the input data, ML classifier may fool and predict the wrong label. If this perturbation is small enough to the human eyes, then the perturbed image can be called an adversarial example [4], [11], [12].

The adversarial example can be obtained by solving the following minimization problem

$$\min \arg \min \|\mathbf{r}\|_2 \quad \text{s.t.} \quad \mathbf{x} + \mathbf{r} \neq C(\mathbf{x}) \quad (1)$$

where \mathbf{r} is adversarial perturbation, $\|\cdot\|_2$ is the Euclidean norm or ℓ_2 norm, \mathbf{x} is the legitimate image (original image), and $C(\cdot)$ yields the classifier’s output label. Based on (1), there are two factors in generating adversarial example, first having minimum perturbation on the legitimate image, and the second, fooling the classifier output.

Misclassification and targeted misclassification attacks are two major goals of adversarial examples. In the misclassification attack, the adversary tries to fool the ML classifier by misclassifying a legitimate example to any different class than the original one. For example, a legitimate image with a label ‘1’ of the MNIST (Modified National Institute of Standards and Technology) dataset would be perturbed in such a way that ML classifier yields an output label belongs to $\{0, 2, 3, 4, 5, 6, 7, 8, 9\}$, yet not ‘1’. In targeted misclassification, the attacker tries to fool the classifier to yield a targeted label. For example, the same image with a label ‘1’ is labeled as a specific number like ‘8’ by the classifier. In this study, we focus on misclassification attacks.

Adversarial examples can be generated based on two different approaches: white-box and black-box. In white-box attacks, the attacker has comprehensive knowledge about the training dataset, model’s parameters, number of CNN layers, loss function, and the whole structure of the model. There are numerous works based on white-box attacks, such as fast gradient sign method (FGSM) [13], deepfool [14], Jacobean-based Saliency Map Attack (JSMA) [15]. For example, FGSM generates an adversarial perturbation for a given legitimate image by computing the gradient of the cost function with respect to the legitimate image of the ML algorithm as follows:

$$\mathbf{x}^* = \mathbf{x} + \epsilon \text{sign}(\nabla_{\mathbf{x}} \mathcal{J}(\mathbf{x}, c)) \quad (2)$$

where ϵ denotes a small scalar value which regulates the perturbation's effect, c is the input label, $\mathcal{J}()$ denotes the model cost function, $\nabla_{\mathbf{x}}$ is the gradient of the trained model with respect to the legitimate image, and $\text{sign}(\cdot)$ is the common mathematical function which yields the sign of its input argument. The common property of white-box attacks is utilizing the model's information for generating the adversarial example.

In contrast, the black-box attack does not have any information about the model's structure and parameters, and training dataset [16]–[19]. This type of attack is more practical because in many cases having access to the training dataset and its labels is not possible. Also, some information such as the model's parameters, number of layers, and loss function may not be public.

Black-box attacks can be separated into three groups: non-adaptive, adaptive and strictly black-box attacks [11]. In a non-adaptive black-box attack, an attacker can have access only to the distribution of the training dataset. In the adaptive black-box case, the attacker does not have any information about the distribution of the dataset, but she can access the target model as an oracle. It means, the attacker can query the output label of legitimate samples as well as adversarial samples. In the strict black-box attack, the attacker does not have access to the training dataset's distribution and an oracle for observing the labels of all legitimate and perturbed samples. But the attacker can have a number of legitimate input samples and their corresponding labels.

Adaptive black-box is more applicable than a non-adaptive case as it does not have any knowledge about the distribution of the training dataset. But, if the number of queries increases the system may detect a probable malicious attack. Besides, some intelligent procedures may be considered to identify the existence of an attack by querying very close samples (legitimate sample and its perturbed versions).

To overcome this issue, Papernot et al. [16] proposed a practical approach for generating adversarial examples based on Jacobian-based dataset augmentation technique to obtain new synthetic training samples. After having an adequate number of samples and corresponding labels, they train a local model and apply a white-box attack (such as FGSM) on this locally trained model to generate adversarial examples. They use the transferability property of ML algorithms [17]. Transferability is a property that enables us to apply adversarial examples generated by a model on another model with the same or different architectures.

The applicability of such attacks mainly revolves around the transferability property of the ML models and having enough large dataset for training the local model. Recently, Hosseini et al. [20] proposed a three-step null labeling method to block the transferability property of the ML models. In the first step, they train the model based on clean data, then they add some perturbation to the input data, and based on

some threshold and probability functions, they assign label 'Null' to the perturbed image. Then, they retrain the model with clean and new adversarial examples which have null labels. This approach enables the model to detect the input adversarial examples by predicting as 'Null'. The previous black-box attacks try to generate adversarial examples based on a white-box approach. In other words, they train a local fake model, then apply a white-box attack to generate adversarial examples.

In [21], the effectiveness of restricting the search for adversarial images to a low frequency domain has been investigated. After focusing on the lower frequency subspace, they randomly perturb the components while restricting the perturbation level. It can be described as adding a low-filtered random noise to the legitimate image. This approach could outperform many black-box attacks. Y. Sharma et al. [22] used discrete cosine transform (DCT) dictionary to map the image into the frequency domain, then they put a hard threshold for choosing LoF components. After transformation into the frequency domain, most of the frequency components have small values and only a few of them have large values. This property of the frequency domain is well known as a sparse representation of an image. Then, by applying perturbations on the LoF components, they could generate faster and more transferable adversarial examples. This approach can completely bypass most of the top-placing defense strategies at the NeurIPS 2017 competition. We motivated by the aforementioned work and used DCT dictionary to transfer images into the sparse (frequency) domain. Then, instead of putting a hard threshold for choosing only k LoF components, we selected k LaS components where some low and high frequency components are picked up. In section II-A, we show the difference between LaS and LoF components.

Focusing on LaS components have been used in many image processing and compression techniques. The JPEG codec [23] takes advantage of this property in order to compress the images. Because, the most critical features and information of an image are available in the LaS components and not just LoF components [23]. Intuitively, since LaS coefficients contain more critical information of an image, image classifiers would also consider those coefficients mostly. We verified this assumption by implementing some experiments (section II-B).

After focusing on LaS components, we propose two scenarios for adding noise. In the first, we randomly perturbed LaS components, and by restricting the perturbation level, the number of required queries to fool the state-of-the-art classifiers were evaluated. Experiment results show that the proposed approach can fool the classifiers with less number of queries compared to the very recent approach which works based on LoF components [22]. In the second scenario, which we call a directed attack, we suppose some number of images from each class are available. Given a legitimate image, we perturb its LaS components in the direction of the most correlated sparse sample from a different class. Our experiments show that this method can successfully fool the state-of-the-art CNN classifiers.

In this study the summary of our contributions are as follow:

- We introduce a black-box approach to generate adversarial examples in the sparse domain in order to fool the ML algorithms such as CNNs, and support vector machine (SVM) classifiers.
- In contrast to the white-box attacks, it does not have any knowledge about the model's structure or the distribution of the training dataset.
- In contrast to the previous black-box attacks, it does not require training a local model for generating adversarial examples. As a result, it does not rely on the transferability property of the state-of-the-art ML algorithms.
- In contrast to the very recent black-box attacks which focused on LoF components, we show that the LaS components can fool the classifiers with a fewer number of queries.
- We proposed an analytical approach to show the relation between adding perturbation in the sparse domain and its effect on the pixel domain.
- We experimented our approach on both grayscale and color image dataset, for different CNN models, and for a discriminative classifier SVM. Experiments show proposed adversarial examples can drastically increase the misclassification rate, and can be considered as a potential threat to the ML classifiers.

II. SPARSITY

Sparsity has been widely used in many applications such as image denoising, deblurring, super resolution, and compression [24]–[29]. It also has been frequently used in biomedical signal processing, because many natural signals are sparse in nature [30]. An image signal $\mathbf{X} \in \mathbb{R}^{p \times q}$ can be reshaped to a vector $\mathbf{x} \in \mathbb{R}^{N=p \times q}$ where N is the number of pixels. Dictionary $\mathbf{D} \in \mathbb{R}^{N \times L}$ is a matrix which linear combination of its columns \mathbf{d}_i can approximately represent the \mathbf{x} as follow

$$\mathbf{x} = \sum_{i \in \{1, 2, \dots, L\}} s_i \mathbf{d}_i = \mathbf{D} \mathbf{s} \quad (3)$$

where $\mathbf{s} \in \mathbb{R}^L$ is the weight vector. If \mathbf{D} provides a weight vector with only k large and $l - k$ negligible or zero elements, then \mathbf{D} and \mathbf{s} can be called as a sparsifying dictionary and sparse representation of input \mathbf{x} , respectively. For brevity, by the rest of this work, we omit the ‘sparsifying’ and refer to the ‘dictionary’ as a sparsifying dictionary. There are some fixed dictionaries based on analytical approaches such as Fourier or wavelet transform which can be designed very fast. In this work, we used DCT dictionary which is an orthonormal matrix ($\mathbf{D} \in \mathbb{R}^{N \times N}$ and $\|\mathbf{d}_i\|_2 = 1$). The coefficients of DCT dictionary can be obtained as follows,

$$d_{i,j} = a_{i,j} \cos \frac{\pi(2i-1)(j-1)}{2N} \quad i, j \in 1, 2, \dots, N$$

$$a_{i,j} = \begin{cases} \sqrt{\frac{1}{N}} & j = 1 \\ \sqrt{\frac{2}{N}} & j \neq 1 \end{cases} \quad (4)$$

where $d_{i,j}$ corresponds to the entry of i th row and j th column of DCT dictionary. Zeroing small sparse coefficients would have negligible effects on the visual information of the image. For example, Fig. 1 illustrates this property. The original image was transferred into the sparse domain via DCT dictionary and forced 70%, 80%, and 90% of its small components to zero, then transformed back into the pixel domain. It is evident that reconstructed images based on only 30%, 20%, or 10% of its LaS components can still preserve lots of visual information of the image.

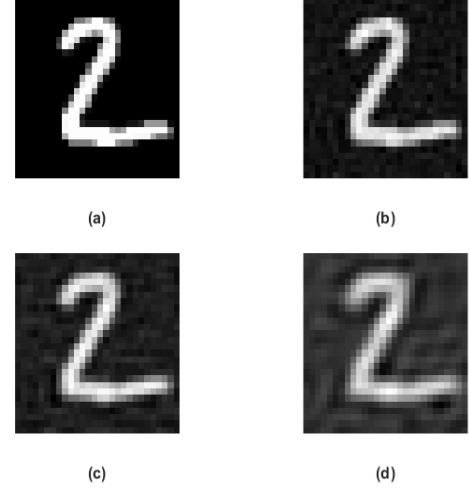


Fig. 1. Transferring image into sparse domain and zeroing small elements of sparse signal: (a) original image, (b) zeroing 70%, (c) 80%, and (d) 90% of small elements.

A. Difference between LaS and LoF components

Sparse domain enables us to get access to the most important part of the information of an image. There are many components that are not common between the LaS and LoF components. Some images may have some information in the middle or even higher frequencies, as a result, they would have LaS components corresponding to the middle or higher frequencies. To evaluate the level of intersection between LaS and LoF components, we used 10,000 color images of size 256x256 pixels. The images had three color channels, and we mapped each channel into the sparse domain, separately. Then we chose $N = (k \times k \times 3)$ LaS and LoF components. For chosen $k = 8$, $k = 16$, and $k = 32$, the number of components are $N = 192$, $N = 768$, $N = 3072$, respectively. Figure 2 shows how many non-intersecting components are available between LaS and LoF components. For $k = 8$, the mean of non-intersecting components is 77, i.e. more than 40% of the LaS components belong to the middle or higher frequencies components. For $k = 16$ and $k = 32$ the mean of non-intersecting components are 229 and 983, i.e. 39% and 32% of the LaS components do not belong to the low frequency space. This experiment shows that the LaS components does not completely overlap with the LoF

components, and a considerable of the information of image signals may belong to the middle of higher frequency bands. In other words, based on a given image, different bands would have different information, as a result, we cannot limit critical information of an image to only its low frequency space. We continued our investigation by evaluating the performance of the CNN models in response to the manipulation of LaS components.

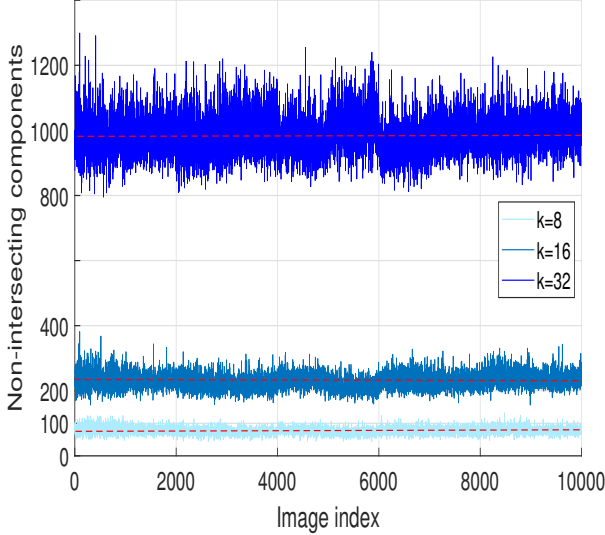


Fig. 2. The number of non-intersecting components of each image.

B. Effect of LaS components on CNN models

Sparse transformation enables us to compact the energy of the signal into a few coefficients. On the other hand, many image classifiers work based on pixel domain and they do not directly consider the sparse domain. A question that may arise here is: “how much manipulating LaS components can impact classifiers’ performance?”. We run some experiments to answer this question and make a connection between the sparse domain and CNNs’ performance. we run our experiments over two classifiers Lenet [31] and ResNet50 [32], with two datasets: MNIST and CIFAR-10. The MNIST dataset is a grayscale handwritten digit that contains a training set of 60,000 samples, and a test set of 10,000 samples. The CIFAR-10 dataset is a color image dataset which contains a training set of 50,000 samples, and a test set of 10,000. Both datasets have 10 different classes and we scaled each sample’s pixels to the range of $[0, 1]$. First, we trained the LeNet with 60,000 samples of MNIST and obtained 98.20% accuracy for 10,000 test samples. In the next step, we mapped all 60,000 training samples into the sparse domain via DCT dictionary and zeroed 99%, 98%, 97%, 96%, 95%, 94%, 93%, and 92% of small components. Then we transformed back these 8 new datasets into the pixel domain. Then we trained the LeNet with these 8 datasets separately, and we calculated their accuracy for the same test dataset (original test dataset without applying

any change in the sparse domain). Results showed that the accuracy of the LeNet classifier does not considerably change (Fig. 3). It can be interpreted that zeroing small components in the sparse domain do not affect the classifier decision process. In other words, the LaS components mostly affect the classification process. For example, as shown in Fig. 3, by zeroing 92% of small sparse components, the accuracy of 97.98% can be achieved which is almost close to the accuracy of the model trained by the original training dataset (98.20%).

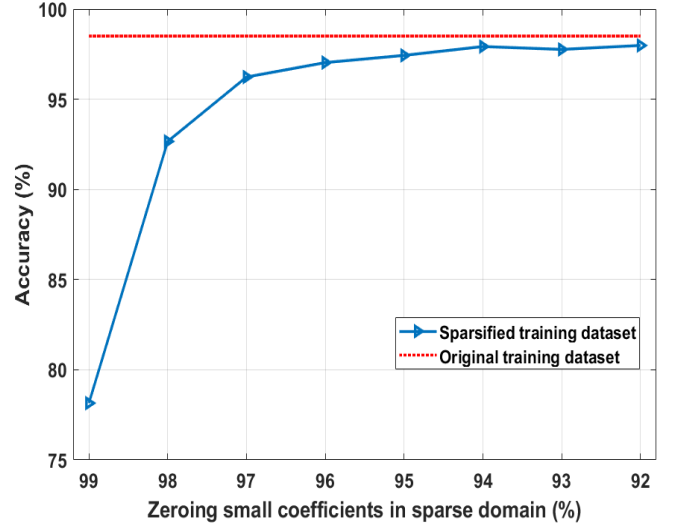


Fig. 3. Effect of Sparsity on LeNet network trained by MNIST dataset.

We run similar experiment over a more complex CNN model (ResNet50) and image dataset, CIFAR-10 which contains different backgrounds. We trained the model from scratch with 50,000 training samples of CIFAR-10, and obtained 92.16% accuracy for 10,000 test samples. Then, all 50,000 training samples were mapped into the sparse domain via DCT dictionary in order to zeroing 95%, 94%, 93%, 92%, 91%, 90%, 80%, and 70% of small components. Then we transformed back these 8 new datasets into the pixel domain. Then, the same network was trained with these 8 datasets separately. Then, we calculated their accuracy for the same test dataset (original test dataset without applying any change in the sparse domain). Figure 4 shows the result of this experiment.

Our experiments showed that even for a complex image dataset and classifier, the small components of sparse domain do not impact classifiers’ decision boundaries. For the brevity, we omitted the results of our experiments over other CNN models which had the same results to verify our assumption.

III. PERTURBING LAS COMPONENTS

In the black-box attack, there is no prior information about the model’s parameters and distribution of the training dataset. We need to evaluate the model output for every query. In other words, some queries should be sent to the model in order to find the minimum or a restricted level of noise that can fool the model. If a method fools the model with a fewer number

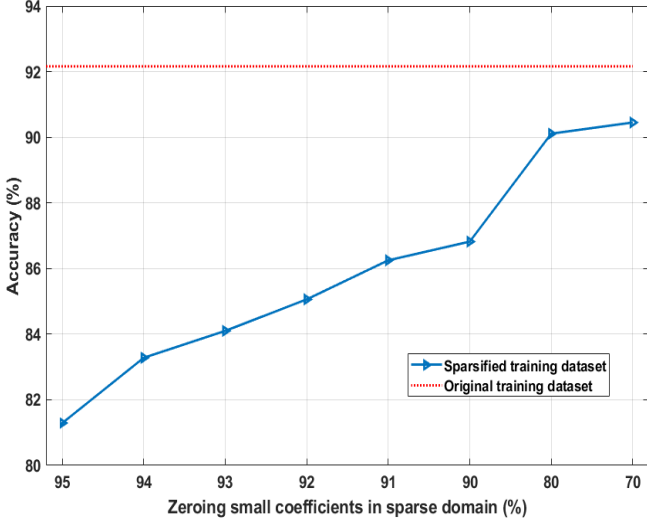


Fig. 4. Effect of Sparsity on ResNet50 network trained by CIFAR-10 dataset.

of queries, that would be more effective. Because, in many cases sending many queries to the server may be identified as a malicious activity and as a result, the new query may be blocked. our experiments showed that LaS components are not the same as the LoF components, and LaS components contain most important visual information of images, and they highly affect the decision boundaries of classifiers. We propose adding restricted noise to LaS components to fool the classifiers.

We run some experiments to show that how our approach is more effective than a very recent approach that adds noise to only LoF components [22]. We used a Gaussian noise with zero mean and variance 1 to generate limited noise. Then we added the noise to the LaS components and compared it with the case that we add noise to the LoF components. We used 10,000 images of CIFAR-10, and resized it to 256x256 pixels. Three CNN models, inceptionV3 [33], ResNet50, and Vgg16 [34] were used to compare the effectiveness of adding noise to the LaS components vs the LoF components. We add noise to the $k = 32$ of LaS and LoF components and defined the MSE less than 0.001 as successful attack. In fig. 5, the histogram of required number of queries to successfully fool the inceptionV3 model is shown. It is evident that LaS components can fool the model with less number of queries. In query less than 10, LaS approach could misclassify 4780 images while LoF approach could misclassify 4024 images. Figures 6 and 7 show similar experiments over ResNet50 and Vgg16 models. For limited query, proposed method could misclassify 5065 images while LoF approach could misclassify 4693 images on ResNet50. Also, based on manipulating LaS components, 4780 images were misclassified by Vgg16, while manipulating LoF components could misclassify 4024 images. We can also observe that the distributions of successful attacks based on our approach are mostly close to the smaller number of queries.

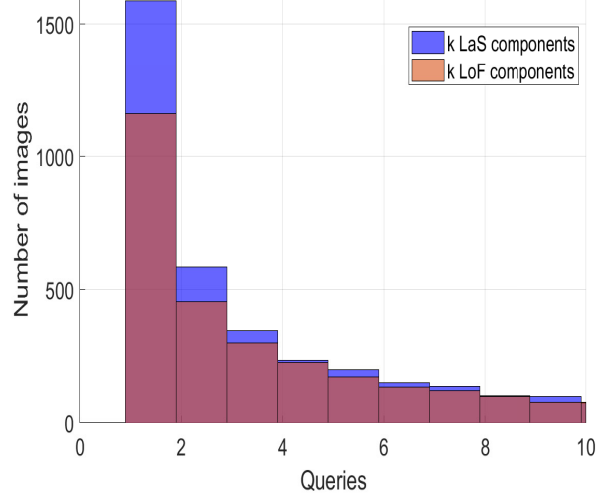


Fig. 5. Distribution of queries for a successful attack on Inception-V3, success defined as perturbation MSE of 0.001 for LaS and LoF approaches, $k = 32$.

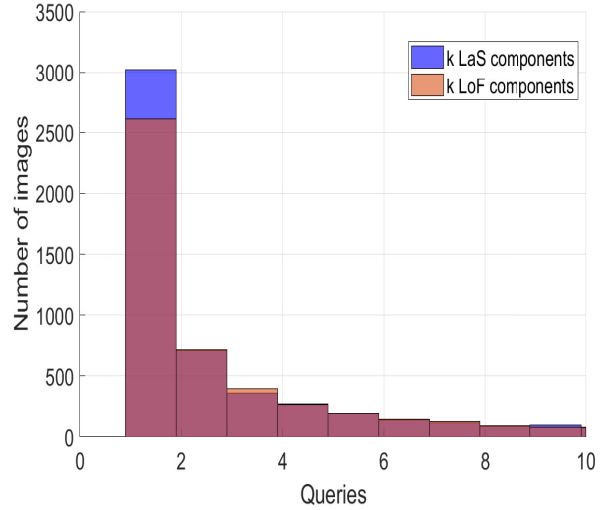


Fig. 6. Distribution of queries for a successful attack on ResNet50, success defined as perturbation MSE of 0.001 for LaS and LoF approaches, $k = 32$.

A. Attacking Google Cloud vision

To evaluate the realistic threat of LaS perturbations, we attack a popular online machine learning service, Google Cloud Vision. The platform provides a TFLite version that can be deployed over Andriod operating system [35]. We used a high-resolution dataset which contained 20938 samples belong to 10 animal “spyder, dog, cat, squirrel, sheep, butterfly, horse, elephant, cow, chicken” [36]. Figure 8 shows the details of the trained model by Google Cloud Vision. We downloaded TFLite version of this model that can be deployed over Android devices in order to apply our attack to this model. Figure 9 shows three samples and corresponding adversarial examples for MSE equals to 0.001, 0.002, and 0.005. The first column shows the legitimate samples that classified correctly

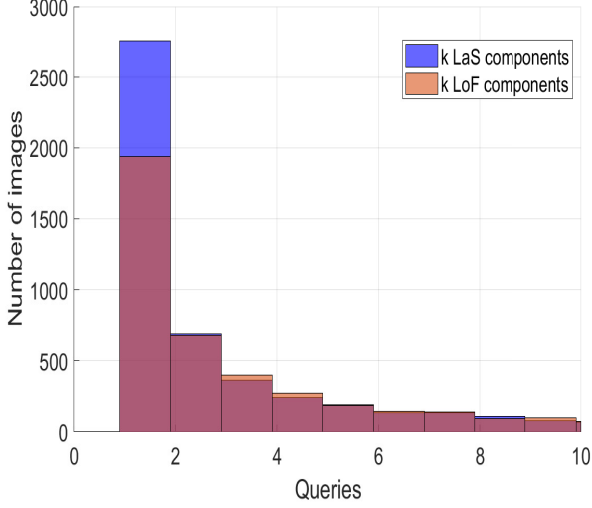


Fig. 7. Distribution of queries for a successful attack on VGG16, success defined as perturbation MSE of 0.001 for LaS and LoF approaches, $k = 32$.

by the classifier, the second column from the left which closed by a green box, belongs to the adversarial examples with $MSE = 0.001$, the other two columns with red boxes related to the adversarial examples with $MSE = 0.002$ and 0.005 . As defined in [22], we set the threshold of $MSE \leq 0.001$ as a successful attack. We released our code and uploaded the TFlite model of google vision API publicly for reproducibility [37].

IV. CASE STUDY: DIRECTED PERTURBATION

In this section, we propose a method for adding noise to the LaS components in order to fool the model into a specific direction. In black-box approach, the attacker can use some samples that have never been used for training stage. Then, the attacker can verify or find the input sample's label by observing the output of the objective model. So, in this section we assume the attacker can have multiple samples of each class and their labels. Suppose the available dataset is $\mathbf{X} = \{\mathbf{x}_i\}_{i=1}^{i=p}$ which contains p samples and each sample belongs to one class out of m available classes, i.e., $C(\mathbf{x}_i) \in \{c_j\}_{j=1}^{j=m}$. We map all samples of the dataset into the sparse domain via DCT dictionary \mathbf{D} . Doing so, $\mathbf{S} = \{\mathbf{s}_i\}_{i=1}^{i=p}$ would be obtained where \mathbf{s}_i is the sparse representation of the \mathbf{x}_i . In the sparse domain, we keep the k LaS components and force the rest of the components to zero. Then each sparse vector is normalized. Doing so, we would have

$$\hat{\mathbf{S}} = \{\hat{\mathbf{s}}_i\}_{i=1}^{i=p}, \|\hat{\mathbf{s}}_i\|_0 = k, \|\hat{\mathbf{s}}_i\|_2 = 1 \quad (5)$$

where $\|\cdot\|_0$ is the zero-norm of a vector which counts the number of non-zero elements of a vector. Sparse vector $\hat{\mathbf{s}}_i$ contains information of the positions and normalized values of the k largest elements of \mathbf{s}_i which belong to class $C(s_i)$. Then for a given $(\hat{\mathbf{s}}_i, C(s_i))$, we find the most correlated sparse vector $(\hat{\mathbf{s}}_j, C(s_j) \neq C(s_i))$. In other words, sparse

vector $\hat{\mathbf{s}}_j$ is the closest sparse vector to the $\hat{\mathbf{s}}_i$, but they belong to different classes. We used the inner product of two vectors $\langle \hat{\mathbf{s}}_i, \hat{\mathbf{s}}_j \rangle$ to calculate the correlation. If we change the k most important elements of $\hat{\mathbf{s}}_i$ with respect to the k most important elements of $\hat{\mathbf{s}}_j$, some information and features of $\hat{\mathbf{s}}_j$ can be transferred into the $\hat{\mathbf{s}}_i$. If some nonzero elements of $\hat{\mathbf{s}}_i$ and $\hat{\mathbf{s}}_j$ have the same positions and close values, there is no need to change them or manipulate them. Because they have common information and changing them cannot help for fooling classifier and may bring unnecessary perturbation in the pixel domain. To prevent this probable issue, we subtract these two vectors to obtain the difference \mathbf{d}_{ij} as follows:

$$\mathbf{d}_{ij} = \hat{\mathbf{s}}_i - \hat{\mathbf{s}}_j \quad (6)$$

Then, we subtract a multiplier of \mathbf{d}_{ij} from the original sparse vector \mathbf{s}_i to obtain sparse adversarial example $\tilde{\mathbf{s}}_i$ as follows:

$$\tilde{\mathbf{s}}_i = \mathbf{s}_i - \delta \mathbf{d}_{ij} \quad (7)$$

where δ is a scalar number that controls the level of directed perturbation. Then, we transfer back the adversarial sparse vector $\tilde{\mathbf{s}}_i$ to the pixel domain via dictionary \mathbf{D} as follows:

$$\tilde{\mathbf{x}}_i = \mathbf{D} \tilde{\mathbf{s}}_i \quad (8)$$

where $\tilde{\mathbf{x}}_i$ is the adversarial example. Through an oracle, we already knew that the response of ML classifier for \mathbf{s}_j is $C(s_j)$, so when adding the elements of $\hat{\mathbf{s}}_j$ to the $\hat{\mathbf{s}}_i$, the classifier may fool and make a wrong classification. By choosing δ and k properly, ML classifier can be fooled.

A. Parameter selection of directed perturbation

Adversarial perturbation on a legitimate image must be imperceptible to the human eye. In other words, an individual by seeing an adversarial example should not be able to detect the fake label. Two scalar parameters k and δ can control the level of perturbation. When we increase these scalars, the level of perturbation in the pixel domain and misclassification rate would be increased accordingly. Two error metrics to compare the adversarial image quality with the legitimate image are the Mean Square Error (MSE) and the Peak Signal to Noise Ratio (PSNR). The MSE yields the cumulative squared error between the adversarial and the legitimate image, whereas PSNR gives a measure of the peak error. The higher the value of PSNR, the higher the quality.

$$MSE = \frac{\|\mathbf{x}_i - \tilde{\mathbf{x}}_i\|_2^2}{N} \quad (9)$$

$$PSNR = 10 \log_{10} \left(\frac{h^2}{MSE} \right) \quad (10)$$

where h is the maximum fluctuation in the input image data type. For example, since we normalize all image dataset to the range of $[0, 1]$, input image's pixels fluctuate between zero and one, so $h = 1$. Before investigating the relation between misclassification rate and quality metrics, we recall two important properties of the matrix-vector multiplications; first, the product of an orthonormal matrix by a vector does not

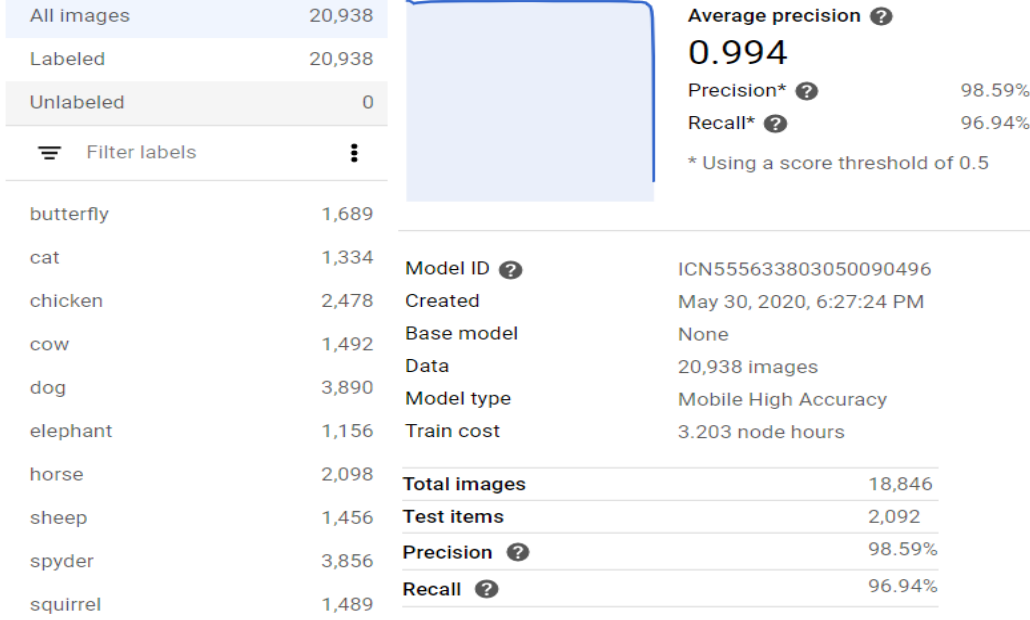


Fig. 8. Information of dataset and trained model by Google Cloud Vision.

change the norm-2 of that vector, and second, a scalar number can take out of the norm-2 of a vector. With respect to these two properties, since $\|\mathbf{x}_i - \tilde{\mathbf{x}}_i\|_2^2 = \|\delta \mathbf{D} \mathbf{d}_{ij}\|_2^2$ and due to the fact that the dictionary \mathbf{D} is an orthonormal dictionary and the δ is a scalar value, $\|\mathbf{x}_i - \tilde{\mathbf{x}}_i\|_2^2 = \delta^2 \|\mathbf{d}_{ij}\|_2^2$. Equation (9) can be further simplified to obtain more straightforward relation between δ and MSE or $PSNR$ in pixel domain as follow

$$MSE = \frac{\delta^2}{N} \|\mathbf{d}_{ij}\|_2^2 = \frac{\delta^2}{N} \|\hat{\mathbf{s}}_i - \hat{\mathbf{s}}_j\|_2^2 = \frac{2\delta^2}{N} (1 - \langle \hat{\mathbf{s}}_i, \hat{\mathbf{s}}_j \rangle) \quad (11)$$

where $\langle \cdot, \cdot \rangle$ is the inner product operation of two vectors. Since both $\hat{\mathbf{s}}_i$ and $\hat{\mathbf{s}}_j$ are normalized vectors, their inner product equals a number belongs to $[-1, 1]$. Hence MSE can be bounded $0 \leq MSE \leq \frac{4\delta^2}{N}$. However, as we choose the two most correlated sparse vectors, their inner product is usually greater than zero. Hence, the upper bound of MSE may be smaller, i.e. $0 \leq MSE \leq \frac{2\delta^2}{N}$. This inequality shows how adding perturbation in the sparse domain can be reflected in the perturbation in the pixel domain. The value of the δ directly affects the MSE . The order of sparsity, k , only has its effect on the inner product. Our simulation results also show that changing the δ can cause more perturbation in pixel domain than changing the k . There is a trade-off between the level of perturbation and the misclassification rate. When we increase the δ or k , more elements of sparse vectors would be involved for perturbation, hence more probability of fooling the ML classifier.

V. EXPERIMENTAL RESULTS OF DIRECTED PERTURBATION

We generated adversarial examples on MNIST and CFAR10 which are common datasets for assessing image classification algorithms. Since our approach is completely independent of

the ML models, adversarial examples were generated for one time. Then we input the examples to the trained CNNs and SVM classifiers to observe how this method can compromise the accuracy of the classifiers. As theoretically was discussed in section IV-A, changing δ and k can generate different adversarial examples with different levels of perturbation. We experimented the obtained MNIST adversarial examples on the LeNet network which works well on digit classification tasks. We trained the network with 60,000 training samples, then the accuracy of the model for 10,000 test samples was 98.2% which means 1.8% misclassification rate. Then we used the same test dataset for generating adversarial examples. We selected 6 different values for the δ and k . It leads to running 36 times, all combinations of δ and k to generate corresponding perturbed test dataset. Then we input all these 36 adversarial sets to the LeNet classifier to observe the response of the network. Figure 10 illustrates how changing the values of δ and k can generate perturbed set and how much it can fool the LeNet classifier. In Fig. 10, left y-axis shows the PSNR value of each perturbed dataset and right y-axis shows the misclassification rate of each perturbed set. Solid blue lines show that PSNR decreases as delta value increases, and dash lines show that the misclassification rate increases as we increase the value of delta.

We tested proposed approach on the SVM classifier as well. We used MNIST dataset, 15000 training and 3000 test samples. We tried all the kernels and found the polynomial kernel as the best kernel to achieve the best score for the model. The misclassification rate of that trained SVM classifier on the benign test dataset was 5%. Then we generated adversarial sets with different levels of perturbations. Figure 11 shows that the SVM classifier is highly sensitive to the proposed directed

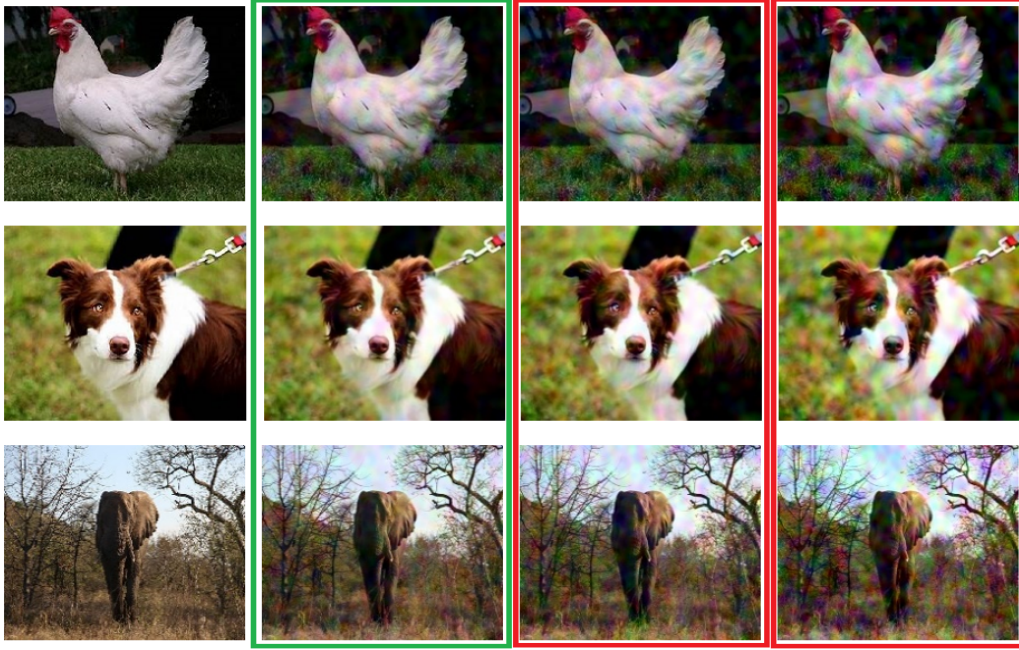


Fig. 9. Samples of attacking Google Cloud Vision. The most left column corresponds to the legitimate image, and the other three columns are misclassified adversarial examples. we supposed $MSE > 0.001$ as a failure and corresponding adversarial examples are bounded by red color boxes. We supposed $MSE = 0.001$ as a success and corresponding examples are enclosed by a green color box.

TABLE I
MISCLASSIFICATION RATE OF RESNET152.

Number of nonzero	$\delta = 0.4$		$\delta = 0.5$		$\delta = 0.6$		$\delta = 0.7$	
	MR(%)	SNR(dB)	MR(%)	SNR(dB)	MR(%)	SNR(dB)	MR(%)	SNR(dB)
k=20	10	17.19	14	15.26	19	13.67	24	12.33
k=30	14	16.31	21	14.37	27	12.78	34	11.45
k=40	19	15.76	26	13.82	35	12.23	42	10.90
k=50	22	15.36	31	13.42	40	11.84	48	10.50

TABLE II
MISCLASSIFICATION RATE OF RESNET50.

Number of nonzero	$\delta = 0.4$		$\delta = 0.5$		$\delta = 0.6$		$\delta = 0.7$	
	MR(%)	SNR(dB)	MR(%)	SNR(dB)	MR(%)	SNR(dB)	MR(%)	SNR(dB)
k=20	14	17.19	18	15.26	23	13.67	28	12.33
k=30	18	16.31	25	14.37	32	12.78	38	11.45
k=40	23	15.76	31	13.82	39	12.23	46	10.90
k=50	26	15.36	36	13.42	44	11.84	52	10.50

attack.

We compared our approach with a recent work by Papernot et al [16]. The Cleverhans Library which has the implementation of their approach was used for comparison [38]. For a fair comparison, we used the same CNN and parameters as they used. We trained the network 10 times, and after each time the misclassification rate of the trained model on both adversarial sets was recorded. Figure 12 shows for $\delta = 15$ and $k = 20$, adversarial examples have a larger misclassification rate than that of the previous work. Also, we calculated the PSNR of both approaches, our method provides higher PSNR which means less perceptible perturbation.

We applied the directed attack over four pre-trained advanced CNN models, Resnet152, Resnet50, InceptionV3, and Vgg16 . We trained the models with 50,000 training samples of CIFAR-10 dataset. Then the output misclassification rates of these models over 10,000 legitimate test samples were obtained, ResNet152 3.57%, ResNet50 5.37%, InceptionV3 4.03%, and Vgg16 12.6%. Then, based on different values of delta and order of sparsity, we generated the adversarial dataset. Tables I and II show the misclassification rate of directed attack to the pretrained ResNet152 and ResNet50 models. Also, Tables III and IV show the effectiveness of our approach for misclassifying InceptionV3 and Vgg16 models.

TABLE III
MISCLASSIFICATION RATE OF INCEPTIONV3.

Number of nonzero	$\delta = 0.4$		$\delta = 0.5$		$\delta = 0.6$		$\delta = 0.7$	
	MR(%)	SNR(dB)	MR(%)	SNR(dB)	MR(%)	SNR(dB)	MR(%)	SNR(dB)
k=20	12	17.19	16	15.26	22	13.67	27	12.33
k=30	16	16.31	23	14.37	31	12.78	38	11.45
k=40	21	15.76	29	13.82	38	12.23	46	10.90
k=50	24	15.36	34	13.42	44	11.84	52	10.50

TABLE IV
MISCLASSIFICATION RATE OF VGG16.

Number of nonzero	$\delta = 0.4$		$\delta = 0.5$		$\delta = 0.6$		$\delta = 0.7$	
	MR(%)	SNR(dB)	MR(%)	SNR(dB)	MR(%)	SNR(dB)	MR(%)	SNR(dB)
k=20	25	17.19	31	15.26	37	13.67	42	12.33
k=30	31	16.31	38	14.37	45	12.78	52	11.45
k=40	36	15.76	44	13.82	52	12.23	59	10.90
k=50	39	15.36	49	13.42	57	11.84	63	10.50

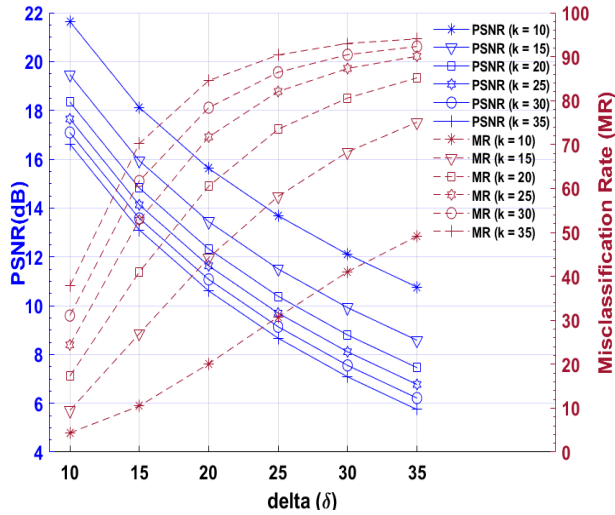


Fig. 10. Generating adversarial examples with different level of perturbation on LeNet.

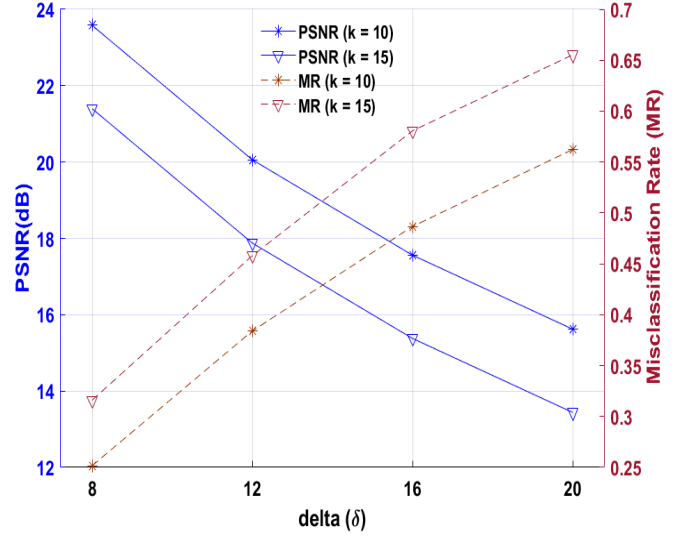


Fig. 11. Generating adversarial examples with different level of perturbation on SVM classifier.

VI. CONCLUSION

In this work, we proposed a new approach for generating adversarial examples by focusing on LaS components of images. We added restricted noise to the LaS components randomly and in a directed approach. By adding perturbation in the sparse domain, two goals could be achieved, first adding the minimum perturbation and the second, adding perturbation to the dominant coefficients of a sparse signal in order to fool the classifier. We did not limit our approach to lower frequency components. Based on a given image, we add perturbation to its LaS components which may contain middle or higher frequency components. In directed attack, we added the noise in the direction of the most correlated sparse vector with a different label. We applied our approach to three image datasets, Animals, MNIST, and CIFAR-10. We applied our approach over Google Cloud Vision platform and

we could successfully fool its trained model. Then, we applied our approach over the state-of-the-art CNN models, namely, Resnet152, Resnet50, InceptionV3, Vgg16, LeNet, and also SVM classifiers. Our simulation results showed that our black-box approach can highly increase the misclassification rate of these classifiers. Also, we compared the proposed approach with recent work, irrespective of the applicability of these two attacks, we found that manipulating LaS components can consistently reduce the query cost, and generate more imperceptible adversarial attacks. In the future, the defense mechanism for this type of attack can be considered and using a different sparsifying basis for generating various adversarial examples can be further investigated.

REFERENCES

- [1] Y. LeCun, B. Boser, J. S. Denker, D. Henderson, R. E. Howard, W. Hubbard, and L. D. Jackel, "Backpropagation applied to handwritten

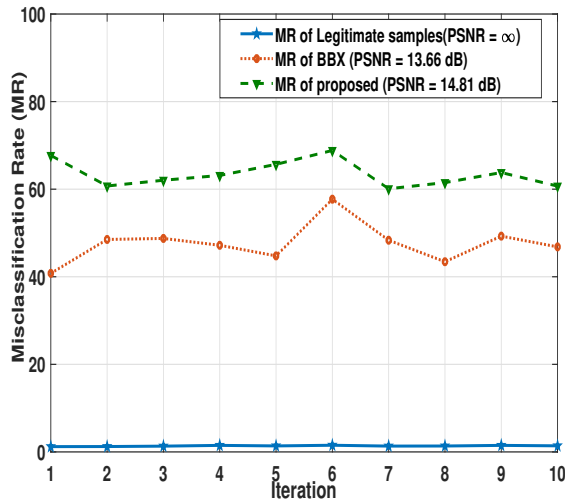


Fig. 12. Comparing the misclassification rate of proposed method of perturbation and recent practical black-box (BBX) approach. [16].

zip code recognition," *Neural Computation*, vol. 1, no. 4, pp. 541–551, Dec 1989.

[2] A. Esteva, B. Kuprel, R. A. Novoa, J. Ko, S. M. Swetter, H. M. Blau, and S. Thrun, "Dermatologist-level classification of skin cancer with deep neural networks," *Nature*, vol. 542, no. 7639, p. 115–118, 2017.

[3] N. Papernot, P. McDaniel, S. Jha, M. Fredrikson, Z. Berkay Celik, and A. Swami, "The Limitations of Deep Learning in Adversarial Settings," *arXiv e-prints*, p. arXiv:1511.07528, Nov 2015.

[4] C. Szegedy, W. Zaremba, I. Sutskever, J. Bruna, D. Erhan, I. Goodfellow, and R. Fergus, "Intriguing properties of neural networks," *arXiv e-prints*, p. arXiv:1312.6199, Dec 2013.

[5] F. Marra, D. Gragnaniello, and L. Verdoliva, "On the vulnerability of deep learning to adversarial attacks for camera model identification," *Signal Processing: Image Communication*, vol. 65, pp. 240 – 248, 2018. [Online]. Available: <http://www.sciencedirect.com/science/article/pii/S0923596518303217>

[6] M. Barreno, B. Nelson, R. Sears, A. D. Joseph, and J. D. Tygar, "Can machine learning be secure?" in *Proceedings of the 2006 ACM Symposium on Information, Computer and Communications Security*, ser. ASIACCS '06. New York, NY, USA: ACM, 2006, pp. 16–25. [Online]. Available: <http://doi.acm.org/10.1145/1128817.1128824>

[7] M. Barreno, B. Nelson, A. D. Joseph, and J. D. Tygar, "The security of machine learning," *Machine Learning*, vol. 81, no. 2, pp. 121–148, Nov 2010. [Online]. Available: <https://doi.org/10.1007/s10994-010-5188-5>

[8] B. Miller, A. Kantchelian, S. Afroz, R. Bachwani, E. Dauber, L. Huang, M. C. Tschantz, A. D. Joseph, and J. Tygar, "Adversarial active learning," in *Proceedings of the 2014 Workshop on Artificial Intelligent and Security Workshop*, ser. AISec '14. New York, NY, USA: ACM, 2014, pp. 3–14. [Online]. Available: <http://doi.acm.org/10.1145/2666652.2666656>

[9] B. Biggio, G. Fumera, and F. Roli, "Security evaluation of pattern classifiers under attack," *IEEE Transactions on Knowledge and Data Engineering*, vol. 26, no. 4, pp. 984–996, April 2014.

[10] N. Papernot, P. McDaniel, A. Sinha, and M. Wellman, "Towards the Science of Security and Privacy in Machine Learning," *arXiv e-prints*, p. arXiv:1611.03814, Nov 2016.

[11] A. Chakraborty, M. Alam, V. Dey, A. Chattopadhyay, and D. Mukhopadhyay, "Adversarial Attacks and Defences: A Survey," *arXiv e-prints*, p. arXiv:1810.00069, Sep 2018.

[12] N. Akhtar and A. Mian, "Threat of Adversarial Attacks on Deep Learning in Computer Vision: A Survey," *arXiv e-prints*, p. arXiv:1801.00553, Jan 2018.

[13] I. J. Goodfellow, J. Shlens, and C. Szegedy, "Explaining and Harnessing Adversarial Examples," *arXiv e-prints*, p. arXiv:1412.6572, Dec 2014.

[14] S.-M. Moosavi-Dezfooli, A. Fawzi, and P. Frossard, "DeepFool: a simple

and accurate method to fool deep neural networks," *arXiv e-prints*, p. arXiv:1511.04599, Nov 2015.

[15] N. Papernot, P. McDaniel, S. Jha, M. Fredrikson, Z. B. Celik, and A. Swami, "The limitations of deep learning in adversarial settings," in *2016 IEEE European Symposium on Security and Privacy (EuroSP)*, March 2016, pp. 372–387.

[16] N. Papernot, P. McDaniel, I. Goodfellow, S. Jha, Z. B. Celik, and A. Swami, "Practical black-box attacks against machine learning," in *Proceedings of the 2017 ACM on Asia Conference on Computer and Communications Security*, ser. ASIA CCS '17. New York, NY, USA: ACM, 2017, pp. 506–519. [Online]. Available: <http://doi.acm.org/10.1145/3052973.3053009>

[17] N. Papernot, P. McDaniel, and I. Goodfellow, "Transferability in Machine Learning: from Phenomena to Black-Box Attacks using Adversarial Samples," *arXiv e-prints*, p. arXiv:1605.07277, May 2016.

[18] N. Narodytska and S. Kasiviswanathan, "Simple black-box adversarial attacks on deep neural networks," in *2017 IEEE Conference on Computer Vision and Pattern Recognition Workshops (CVPRW)*, July 2017, pp. 1310–1318.

[19] I. Rosenberg, A. Shabtai, L. Rokach, and Y. Elovici, "Generic Black-Box End-to-End Attack Against State of the Art API Call Based Malware Classifiers," *arXiv e-prints*, p. arXiv:1707.05970, Jul 2017.

[20] H. Hosseini, Y. Chen, S. Kannan, B. Zhang, and R. Poovendran, "Blocking Transferability of Adversarial Examples in Black-Box Learning Systems," *arXiv e-prints*, p. arXiv:1703.04318, Mar 2017.

[21] C. Guo, J. S. Frank, and K. Q. Weinberger, "Low Frequency Adversarial Perturbation," in *Conference on Uncertainty in Artificial Intelligence (UAI)*, 2019.

[22] Y. Sharma, G. W. Ding, and M. A. Brubaker, "On the Effectiveness of Low Frequency Perturbations," in *Proceedings of the Twenty-Eighth International Joint Conference on Artificial Intelligence*, 2019, pp. 3389–3396.

[23] G. K. Wallace, "The JPEG still picture compression standard," *IEEE Transactions on Consumer Electronics*, 1992, vol. 38, no.1, pp. xviii–xxxiv.

[24] M. Elad and M. Aharon, "Image denoising via sparse and redundant representations over learned dictionaries," *IEEE Transactions on Image Processing*, vol. 15, no. 12, pp. 3736–3745, Dec 2006.

[25] S. Ujan, S. Ghorshi, M. Pourebahram, and S. A. Khoshnevis, "On the use of compressive sensing for image enhancement," in *2016 UKSim-AMSS 18th International Conference on Computer Modelling and Simulation (UKSim)*. IEEE, 2016, pp. 167–171.

[26] Haichao Zhang, Jianchao Yang, Yanning Zhang, and T. S. Huang, "Sparse representation based blind image deblurring," in *2011 IEEE International Conference on Multimedia and Expo*, July 2011, pp. 1–6.

[27] J. Yang, J. Wright, T. S. Huang, and Y. Ma, "Image super-resolution via sparse representation," *IEEE Transactions on Image Processing*, vol. 19, no. 11, pp. 2861–2873, Nov 2010.

[28] J. Zepeda, C. Guillemot, and E. Kijak, "Image compression using sparse representations and the iteration-tuned and aligned dictionary," *IEEE Journal of Selected Topics in Signal Processing*, vol. 5, no. 5, pp. 1061–1073, Sep. 2011.

[29] R. G. Baraniuk, "Compressive sensing [lecture notes]," *IEEE Signal Processing Magazine*, vol. 24, no. 4, pp. 118–121, July 2007.

[30] S. A. Khoshnevis and S. Ghorshi, "Recovery of event related potential signals using compressive sensing and kronecker technique," in *7th IEEE Global Conference on Signal and Information Processing (GlobalSIP)*, Ottawa, Canada, 2019.

[31] Y. LeCun, P. Haffner, L. Bottou, and Y. Bengio, "Object recognition with gradient-based learning," in *Shape, Contour and Grouping in Computer Vision*. London, UK, UK: Springer-Verlag, 1999, pp. 319–. [Online]. Available: <http://dl.acm.org/citation.cfm?id=646469.691875>

[32] K. He, X. Zhang, S. Ren, and J. Sun, "Deep Residual Learning for Image Recognition," *arXiv e-prints*, p. arXiv:1512.03385, Dec 2015.

[33] C. Szegedy, V. Vanhoucke, S. Ioffe, J. Shlens, and Z. Wojna, "Rethinking the Inception Architecture for Computer Vision," *arXiv e-prints*, p. arXiv:1512.00567, 2015.

[34] K. Simonyan and A. Zisserman, "Very Deep Convolutional Networks for Large-Scale Image Recognition," *arXiv preprint*, p. arXiv:1409.1556, 2014.

[35] Google, "Deploy machine learning models on mobile and iot devices," Available: <https://www.tensorflow.org/lite>. [Accessed: 02-April-2020].

[36] <https://www.kaggle.com/alessiocorrado99/animals10>

- [37] <https://github.com/hadizand/Adversarial-examples.git>
- [38] N. Papernot, F. Faghri, N. Carlini, I. Goodfellow, R. Feinman, A. Kurakin, C. Xie, Y. Sharma, T. Brown, A. Roy, A. Matyasko, V. Behzadan, K. Hambardzumyan, Z. Zhang, Y.-L. Juang, Z. Li, R. Sheatsley, A. Garg, J. Uesato, W. Gierke, Y. Dong, D. Berthelot, P. Hendricks, J. Rauber, and R. Long, "Technical report on the cleverhans v2.1.0 adversarial examples library," *arXiv preprint arXiv:1610.00768*, 2018.